

Validation of In-field Calibration for Low-Cost Sensors Measuring Ambient Particulate Matter in Kolkata, India

Siddharth Nobell¹, Arnab Majumdar¹, Shovon Mukherjee¹, Sukumar Chakraborty¹, Sanjoy Chatterjee¹, Soumitra Bose¹, Anindita Dutta^{2,3}, Sandhya Sethuraman³, Daniel M. Westervelt⁴, Shairik Sengupta⁵, Rakhi Basu^{6,7}, V. Faye McNeill^{3,8*}

¹ Envirome Research, Kolkata 700091, INDIA

² Department of Medicine, University of Chicago, Chicago, IL USA

³ Department of Chemical Engineering, Columbia University, New York, New York 10027, USA

⁴ Lamont-Doherty Earth Observatory, Columbia University, Palisades, New York, USA

⁵ Indian Institute of Science, Bangalore 560012, INDIA

⁶ The World Bank Group, Washington, D.C., USA

⁷ Conveh, Irvine, California, USA

⁸ Department of Earth and Environmental Sciences, Columbia University, New York, New York 10027, USA

* Corresponding author. +1 212-854-2869 vfm2103@columbia.edu

Abstract

Low-cost sensors (LCS) provide opportunities for neighborhood-level air pollution data collection, yet significant knowledge gaps remain regarding the accurate application and interpretation of LCS. In this study, we present an in-field calibration of a network of 20 low-cost ambient particulate matter sensors (LCS) in greater Kolkata, India, operating between October 2018-April 2019. In order to understand LCS performance in relation to local reference-grade PM_{2.5} monitors (RGMs), three of these LCS were co-located with RGMs operated by the West Bengal Pollution Control Board at Rabindra Bharati University (RBU), Victoria Memorial (VICTORIA), and Padmapukur (Howrah, PDM). Data from the co-locations were used to calibrate the LCS network using random forest regression and multiple linear regression approaches. Measured relative humidity and temperature were significant model features. Agreement between the LCS and RGM for 24-h averaged PM_{2.5} measurements was strongest at RBU, with an uncalibrated root mean squared error (RMSE) of 27.1 $\mu\text{g m}^{-3}$, followed by PDM (32.6 $\mu\text{g m}^{-3}$) and VICTORIA (50.7 $\mu\text{g m}^{-3}$). Multiple linear regression was used to derive calibration models. Cross-calibration between co-located LCS-RGM pairs was tested. The LCS data after cross-calibration correctly identified days as being in or out of attainment with the 24h National Ambient Air Quality Standard of 60 $\mu\text{g m}^{-3}$ 91% of the time. The corrected data accurately identifies days with an India scale Air Quality Index of “poor” or worse 94% of the time. This suggests that LCS can be a useful supplement to RGM networks for air quality management. Diurnal trends and a high level of correlation across the hybrid LCS-RGM network suggest regional and secondary sources of PM_{2.5} are important in Kolkata.

Keywords: Air Pollution, Air Quality, Atmospheric Aerosols, PM_{2.5}, Urban Aerosols

47

48 **1 INTRODUCTION**

49

50 Ambient air pollution is a major environmental health issue. Atmospheric fine particulate matter,
51 or PM_{2.5} (particles with aerodynamic diameters less than 2.5 micrometers), is one of the leading
52 causes of premature mortality and morbidity worldwide (Cohen et al., 2017). PM_{2.5} exposure
53 causes an estimated 1.56-year decrease in life expectancy in South Asia, more than in any other
54 region (Apte et al., 2018). Although the World Health Organization has set guideline values for
55 PM_{2.5} at 5 µg m⁻³ annual mean and 15 µg m⁻³ 24-hour mean, pollutant levels remain many-fold
56 higher than this value in most places, particularly in low- and middle-income countries (LMICs)
57 (WHO, 2021). Continuous measurements of PM_{2.5} are needed in order to establish baseline
58 conditions, quantify the local negative impacts of pollution, identify pollution sources, plan policies
59 to comply with set air quality goals, and track air quality improvements (McNeill, 2019; World
60 Bank, 2017). While the density of ground-based reference-grade PM_{2.5} monitors across India has
61 increased since 2016 under the National Air Quality Monitoring Programme (CPCB, 2022;
62 Sethuraman et al., 2021; McNeill and Nunes, 2017), data are not yet available at high spatial
63 resolution. Low-cost sensors (LCS) provide opportunities for neighborhood-level data collection,
64 enabling the identification of air pollution “hotspots” and the quantification of local health impacts
65 (Pinder et al., 2019). LCS are lower-fidelity sensors that generally operate on optical principles for
66 PM_{2.5} detection and require less power and maintenance than reference-grade monitors (RGMs).

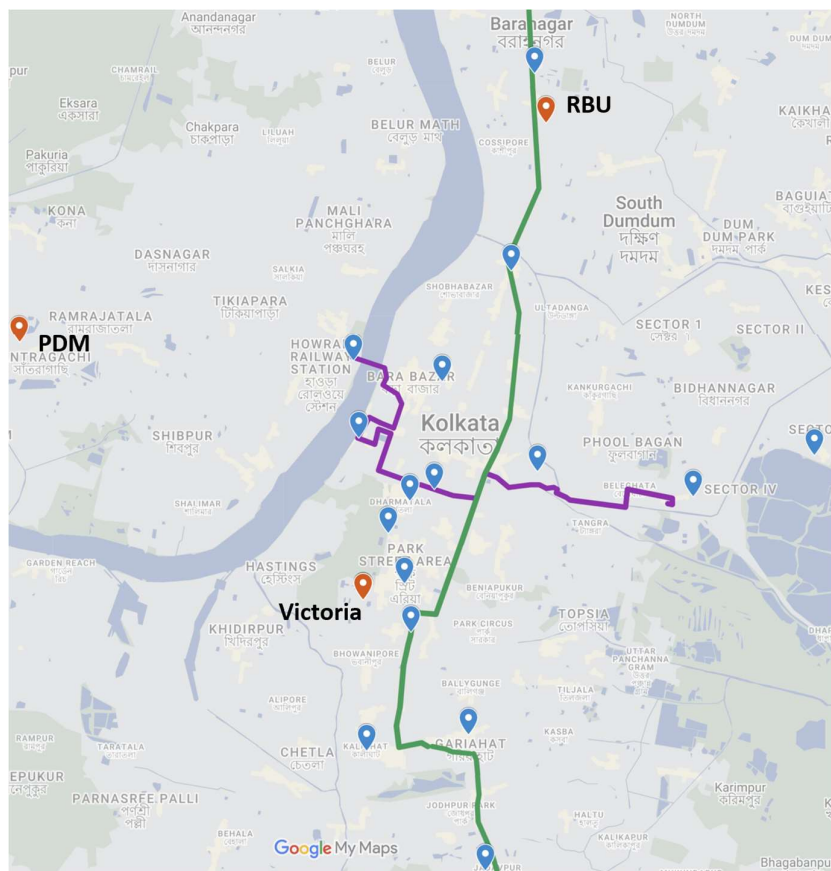
67 Although the use of LCS for air pollution monitoring and air pollution research has proliferated
68 in the past decade, significant knowledge gaps and caveats remain regarding the accurate
69 application and interpretation of LCS (Malings et al., 2020; Giordano et al, 2021; Hagler et al.,
70 2018). LCS that measure ambient PM_{2.5} often underperform under the environmental conditions
71 typical of air pollution events in India (high humidity, high pollution loadings, light-absorbing
72 particles) (Di Antonio, et al., 2018; Jayaratne et al., 2018). Sensor performance may also degrade

73 in harsh environments (Amegah, 2018). The impact of environmental conditions and particle
74 characteristics such as size, shape, and composition on different LCS technology remains a
75 knowledge gap.

76 In-field calibration of LCS sensors has emerged as a solution for improving the accuracy of data
77 from LCS networks (Malings et al., 2020; Giordano et al, 2021). Including RGMs in an air quality
78 network provides a reference for LCS calibration. By co-locating LCS and RGMs, a calibration for
79 the LCS network may be developed. Several studies have focused on local calibrations of LCS
80 distributed in the U.S. (Malings et al., 2020; Zimmerman et al., 2018) and African cities (McFarlane
81 et al, 2021a,b; Raheja et al., 2022) with machine learning approaches, but to date this approach has
82 had limited application in urban environments in India (Gupta et al., 2022).

83 In this manuscript, we describe a sensor network deployed by Enviome Research in collaboration
84 with The World Bank between October 2018 and January 2019 in central Kolkata, India, which
85 collected data until summer 2019. The network consisted of twenty low cost PM_{2.5} sensors (Clarity,
86 Inc.), and included three co-locations with reference grade PM_{2.5} monitors under the operation of
87 the West Bengal Pollution Control Board (WBPCB). The design of this network allowed for the
88 analysis of the performance of these light-scattering based LCS in the Indian urban environment.
89 Using the network, we were able to establish a baseline assessment of local air quality along two
90 major transportation corridors targeted for transition to electric vehicle public transportation
91 (World Bank, 2020) (Fig. 1). The multiple co-locations also enabled a robust test of the principle
92 of field calibration by allowing calibration and cross-check across co-location pairs.

93



94
95
96
97
98

Figure 1. Sensor placement. Markers indicate the locations of Clarity Monitors. Red markers indicate Clarity Monitors co-located with WBPCB reference grade PM_{2.5} monitors. S12 (purple) and S9 (green) bus routes are indicated. See text for details. Background map © Google, 2023

99

2. NETWORK DESCRIPTION AND METHODOLOGY

100

101 In this section, we describe the sensors, the network design, and the analysis approach. Twenty

102 Clarity Node S air quality monitors were deployed in Kolkata and Howrah, India starting in Fall

103 2018 (Fig. 1). Table 1 provides a complete list of sensor locations. The sensor network was

104 designed to characterize baseline air pollution levels along the two busiest bus corridors in central

105 Kolkata, and to compare LCS performance to RGMs in three areas of the city. The bus corridors

106 studied were route S9 (Belgharia to Jadavpur) and S12 (Newtown to Howrah), which span across

107 the city from far North to South, and far East to West. Clarity Node S devices were placed at 2-3

108 km intervals along these routes. Five more Clarity Node S devices were placed near existing PM_{2.5}

109

110 **Table 1.** Sensor Network Details.

Code	Area	Lat (N), Lon (E)	Note
Victoria Memorial (VICTORIA)	Central, S9 Route	22.543529, 88.345144	Installed Nov 30, 2018 WBPCB Co-location
Esplanade	Central, S12 Route	22.560900, 88.354100	Installed Oct 9, 2018
Marble Palace	Central	22.58206, 88.360217	Installed Oct 30, 2018
Camac Street	Central	22.546349, 88.353041	Installed Oct 30, 2018
Park Street Crossing	Central, S12 Route	22.555199, 88.349983	Installed Oct 30, 2018
Wellington	Central, S12 Route	22.562954, 88.358787	Installed Oct 30, 2018
Belehata	East, S12 Route	22.561763, 88.408248	Installed Oct 30, 2018
SDF Building	East, S12 Route	22.569032, 88.431324	Installed Oct 6, 2018
Sealdah Sales Tax	East, S12 Route	22.566107, 88.378469	Installed Oct 7, 2018
Padmapukur (PDM)	Howrah	22.58898, 88.279613	Installed Nov 30, 2018 WBPCB Co-location
Howrah Bus Depot	Howrah, S12 Route	22.585611, 88.343274	Installed Oct 9, 2018
Ghusuri	Howrah	22.611539, 88.347443	Installed Oct 26, 2018
Rabindra Bharati University (RBU)	North	22.627875, 88.3804	Installed Jan 1, 2019 WBPCB Co-location
Belgharia Police Station	North, S9 Route	22.658795, 88.376852	Installed Oct 30, 2018
Shyambazar	North, S9 Route	22.601706, 88.373702	Installed Oct 30, 2018
Baranagar Police Station	North, S9 Route	22.636537, 88.378087	Installed Oct 30, 2018
Elgin & Lansdowne	South, S9 Route	22.537756, 88.354285	Installed Oct 30, 2018
Gariahat	South, S9 Route	22.519741, 88.365247	Installed Oct 26, 2018
Jadavpur (8B bus stand)	South, S9 Route	22.495761, 88.368469	Installed Oct 7, 2018
Rashbehari Crossing	South, S9 Route	22.516881, 88.345842	Installed Oct 30, 2018
Millenium Park	West, S12 Route	22.571949, 88.344400	Installed Oct 30, 2018

111

112 RGMs (WBPCB and U.S. Diplomatic Post). Out of the five devices, three were placed in
113 sufficiently close proximity to the RGMs (i.e., on the enclosures housing the RGMs) to be
114 considered co-located for calibration purposes. These three were PDM: Padmapukur, RBU:

115 Rabindra Bharati University, and VICTORIA: Victoria Memorial. Sensors were installed 12-18
116 feet from the ground. Each Clarity Movement Node S monitor consisted of a Plantower PMS 6003
117 dual laser light scattering PM sensor, an NO₂ electrochemical cell sensor (110-508, SPEC Sensors),
118 and a Bosche BME280 sensor to estimate pressure, relative humidity (RH), and temperature (T)
119 inside the sensor housing. The Node S reported measurements of PM_{2.5}, PM₁₀, NO₂, RH, and T at
120 a default frequency of 15 minutes and uploaded the data via cellular signal to the Clarity cloud
121 system. Data were processed, including data cleaning, by Clarity prior to data storage in the Clarity
122 Cloud. No additional cleaning of Clarity data was performed in this study; data were used as
123 received from the Clarity Dashboard. The present analysis focuses on the PM_{2.5} data. The Clarity
124 sensors were co-located as a group in a controlled environment in Kolkata (SDF building) and
125 checked for consistent performance prior to deployment.

126 WBPCB PM_{2.5} monitors (RGMs) are Beta Attenuation Monitors (MP101M, Envea Global).
127 These instruments were housed in enclosures roughly 4.2 m × 3.5 m × 2.5 m high (WBPCB, 2018).
128 Co-located LCS were installed on poles extending 3-4 feet from the roof of these enclosures. The
129 RGMs collected sample data every fifteen minutes and uploaded the data to the online data
130 collection and reporting web portal as hourly average. WBPCB instruments are certified on a 24-
131 hour basis. WBPCB performed data cleaning prior to storage, but we also screened for values of 0
132 and 999 μg m⁻³ from the WBPCB datasets (<1% of data points). These values were discarded before
133 averaging and further analysis.

134 Calibration analysis was performed using the scikit-learn package in Python (Müller and Guido,
135 2017). Basic features of the datasets included PM_{2.5} measured by RGM and Clarity Monitor, as
136 well as T and RH measured by the Clarity Monitor. Regression was performed for individual co-
137 located Clarity-RGM pairs using Clarity PM_{2.5}, T, and RH as explanatory variables. The 24-hr
138 averaged datasets consisted of 188 (i.e., 24-hr averages for 188 days) and 194 points for RBU and

139 PDM, respectively. A 75:25 train:test split implemented via random distribution was used. The
140 generalizability of the calibration was tested by cross-calibrating between Clarity-RGM pairs (i.e.,
141 train dataset from co-location pair 1, test data from co-location Clarity Monitor 2, compared result
142 to the location 2 RGM). Additional details are available in the Results section.

143 The algorithms tested for calibration were multiple linear regression and Random Forest
144 regression. Random Forest regression is attractive for this application because it is powerful while
145 making it possible to avoid overfitting. Multiple linear regression, if it provides enough accuracy,
146 is valuable in that it produces an analytical expression for the calibration as follows, simplifying
147 calibration of the wider network (Malings et al., 2020; McFarlane et al., 2021a):

148

$$149 \quad \text{PM}_{2.5, \text{corrected}} = \beta_0 + \beta_1 \times \text{Clarity PM}_{2.5} + \beta_2 \times T \text{ (}^\circ\text{C)} + \beta_3 \times \text{RH (\%)} \quad (1)$$

150

151 Where the β_i are fitting parameters. The default settings in `scikit_learn` were applied for
152 `linear_model.LinearRegression()` (Müller and Guido, 2017). For
153 `RandomForestRegressor()`, we used 100 estimators, a maximum tree depth of 10, 10
154 minimum samples required to be a leaf node, and a fixed random state of 5.

155 The raw data and the regression results were evaluated based on their agreement with the
156 WBPCB reference data, as measured by the coefficients of determination (r^2) and the root mean
157 squared error (RMSE), and the normalized RMSE (NRMSE). RMSE is calculated according to:

$$158 \quad \sqrt{\frac{\sum_{i=0}^n (x_i - \hat{x}_i)^2}{N}} \quad (2)$$

159 where x_i is the series of observed values, \hat{x}_i is the expected value, and N is the number points in the
160 series. NRMSE, a unitless metric, is calculated by normalizing the RMSE with the range of the
161 variable, i.e.

162
$$NRMSE = \frac{RMSE}{x_{high}-x_{low}} \quad (3)$$

163 The corrected data were also evaluated for their accuracy in diagnosing a day as in or out of
164 attainment with the Indian 24h National Ambient Air Quality Standard (NAAQS) of $60 \mu\text{g m}^{-3}$, or
165 placing the day in the correct Indian Air Quality Index (AQI) category.

166 Spatial variability in the data was analyzed by calculating the Pearson correlation
167 coefficient, r , between datasets obtained at different sites. For datasets A and B,

168
$$r_{AB} = \frac{1}{N-1} \sum_{i=1}^N \left(\frac{A_i - \mu_A}{\sigma_A} \right) \left(\frac{B_i - \mu_B}{\sigma_B} \right) \quad (4)$$

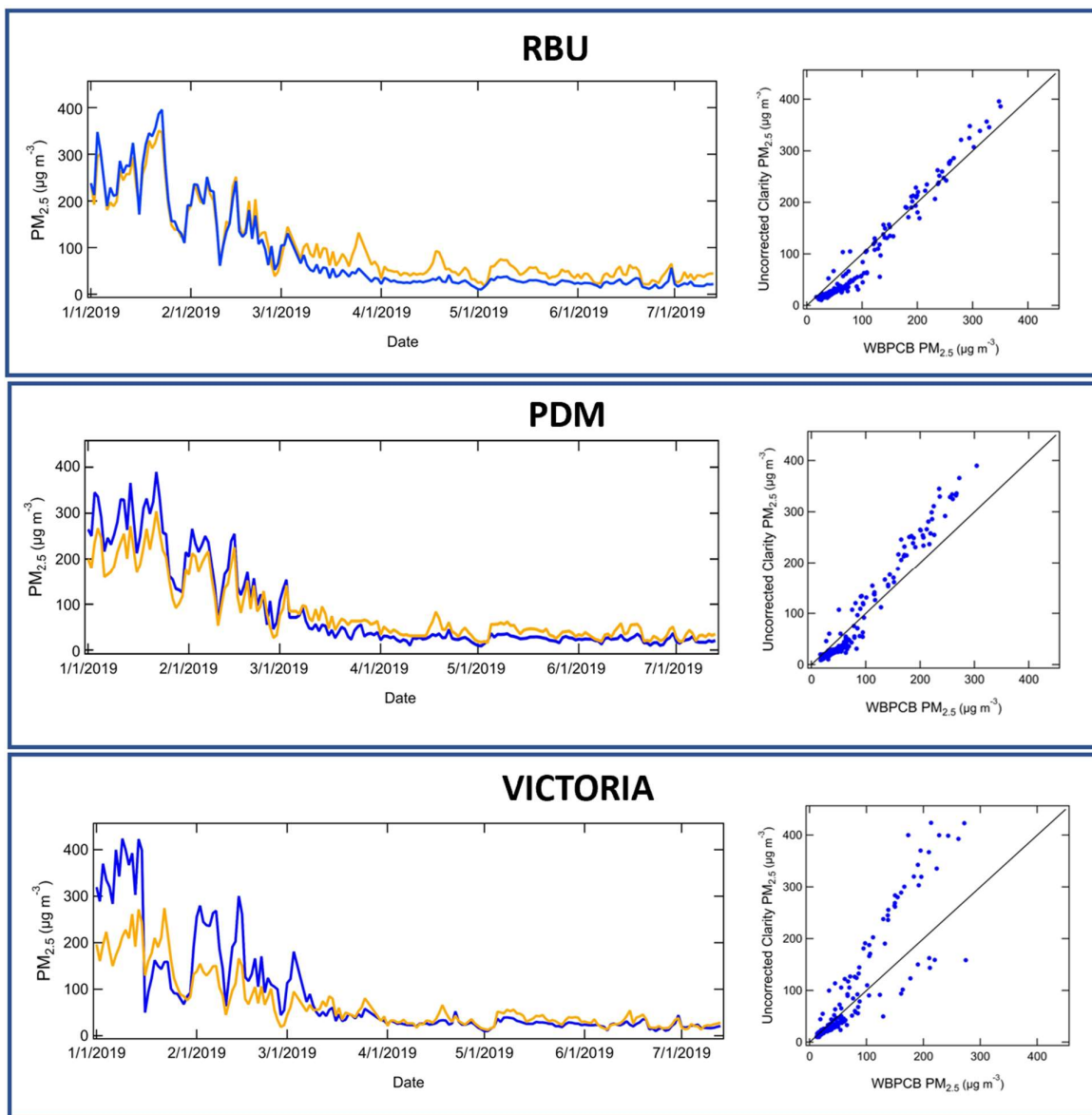
169 where N is the size of each dataset, μ_j is the mean, and σ_j is the standard deviation.

170

171 3. RESULTS

172

173 Data collection spanned the post-monsoon season 2018 (October-November), winter 2018/2019
174 (December-February), and spring/summer 2019 (March-July). Sensor installation took place
175 between November 2018-January 2019 (Table 1). Comparisons between the WBPCB RGM data
176 and the uncorrected Clarity data at the three co-location sites are shown in Fig. 2. We used 24-hour
177 averaged data since this is the basis upon which the RGM was certified. Typical of Plantower-
178 based instruments, the Clarity sensors showed qualitative agreement with the RGMs, with some
179 high bias for higher $\text{PM}_{2.5}$ loadings ($>100 \mu\text{g m}^{-3}$). Agreement between the LCS and RGM was
180 strongest at RBU, with an uncalibrated RMSE of $27.1 \mu\text{g m}^{-3}$ (NRMSE = 0.070), followed by PDM
181 (RMSE = $32.6 \mu\text{g m}^{-3}$, NRMSE = 0.086) and VICTORIA (RMSE = $50.7 \mu\text{g m}^{-3}$, NRMSE = 0.122).
182 The RBU site is located inside the university campus, away from traffic and other sources (167 m
183 away from the nearest major roadway). PDM is in a primarily residential area near a pond, 15 m
184 from a minor roadway, 167 m from a major roadway, and 373 m from the Mumbai-Kolkata



185

186 **Figure 2.** 24-hr averaged PM_{2.5} data from WBPCB RGMs (orange) and uncorrected Clarity
 187 Monitor data (as received from Clarity Cloud) (blue) for the RBU, PDM, and VICTORIA co-
 188 colocations during the study period. 1:1 lines are shown on the right hand panels as a guide to the
 189 eye. Refer to Table 2 and Table 3 for performance metrics.

190

191 Highway. VICTORIA is in a centrally located green zone near a pond, near a minor roadway, and
 192 200-230 m from two major roadways, so, humidity and local source effects are possible. PDM and
 193 VICTORIA showed higher average RH than the rest of the network. Only the RBU and PDM

194 datasets were used for calibration analysis due to the lower Clarity-RGM agreement and higher
195 variability in the Clarity data at VICTORIA.

196 In order to investigate the sensitivity of the sensor performance to environmental factors, we
197 analyzed the Clarity:RGM agreement after splitting the dataset based on RH and/or PM_{2.5} levels
198 (Table 2). This analysis was done using hourly averaged data in order to capture diurnal variations
199 in RH. Performance of Plantower-based sensors has been reported to degrade for RH > 75%
200 (Jayaratne et al., 2018). We split the RBU, PDM, and VICTORIA datasets into RH >75% and
201 RH<75% groups. The results varied by co-location site, with VICTORIA showing significant
202 degradation in sensor performance for RH>75%. PDM also showed worse Clarity:RGM agreement
203 for RH >75%, although the difference was not as great as observed at VICTORIA. No significant
204 RH effect was observed at RBU.

205

206 **Table 2.** Uncorrected Clarity node:RGM agreement for the three co-location sites. Shown are root
207 mean squared error (RMSE ($\mu\text{g m}^{-3}$)) and normalized RMSE (NRMSE, unitless, in parentheses),
208 on 24 hr or hourly averaging basis, and for the full dataset, or segregated based on relative humidity
209 level or fine particle mass loading.

210

<i>Location</i>	RMSE ₂₄	RMSE _{hourly}	RMSE _{hourly} RH>75%	RMSE _{hourly} RH<75%	RMSE _{hourly} PM _{2.5} >100 $\mu\text{g m}^{-3}$	RMSE _{hourly} PM _{2.5} <100 $\mu\text{g m}^{-3}$
RBU	27.1 (0.070)	44.7 (0.091)	40.0 (0.081)	46.8 (0.136)	70.0 (0.142)	31.5 (0.350)
PDM	32.6 (0.086)	55.0 (0.112)	68.1 (0.139)	39.2 (0.116)	101 (0.207)	24.1 (0.268)
VICTORIA	50.7 (0.123)	74.9 (0.181)	100 (0.242)	44.2 (0.147)	155 (0.375)	18.4 (0.204)

211

212

213 Splitting the dataset on PM_{2.5} = 100 $\mu\text{g m}^{-3}$ showed significantly better Clarity:RGM agreement
214 for lower PM_{2.5} loadings, and worse sensor performance for higher loadings, for all three co-
215 location sites (Table 2). Deterioration of sensor performance for high PM_{2.5} loadings >100 $\mu\text{g m}^{-3}$
216 is consistent with studies of low-cost optical particle counter performance in Delhi (Crilley, et al.

217 2020) and Plantower PMS3003 sensors in Kanpur (Zheng, et al. 2018). Seasonal variation in $PM_{2.5}$
218 in Kolkata is strong enough that splitting the data at $PM_{2.5} = 100 \mu g m^{-3}$ is effectively similar to
219 segregating the data by seasons, since loadings are generally $<100 \mu g m^{-3}$ outside the post-monsoon
220 and winter seasons (Fig. 2). There are many other reasons to characterize sensor performance with
221 the changing seasons, including varying meteorological conditions, varying sources, and possible
222 degradation of sensor performance with time. However, because of the timing of the sensor
223 deployment in this study (deployment beginning in post-monsoon, when $PM_{2.5}$ is high, and ending
224 in summer, when $PM_{2.5}$ is lower), it is difficult to distinguish the effects of these influences on the
225 sensor performance from the strong effect of $PM_{2.5}$ loading.

226 Random Forest (RF) and Multiple Linear Regression (MLR) analyses were performed on the
227 24-hr averaged RBU and PDM datasets, because the WBPCB monitors are certified on a 24 hour
228 basis. Factors tested were $PM_{2.5}$, T, and RH (Table 3). $PM_{2.5}$ was the most significant explanatory
229 variable in the RF regression, followed by RH and T, consistent with the results of the data
230 segregation analysis (Table 2). The RF and MLR approaches yielded similar satisfactory agreement
231 with the reference data for both co-location sites, with $R^2 > 0.9$ in each case. Since MLR yields an
232 analytical expression for the calibration model, which is straightforward to apply to the rest of the
233 sensor network, MLR was used in the remainder of the study.

234 Malings et al. (2020) used a piecewise MLR approach for Pittsburgh, USA data, splitting the
235 data at $PM_{2.5} = 20 \mu g m^{-3}$. We tested this approach, splitting the data at $PM_{2.5} = 100 \mu g m^{-3}$. Using
236 24-hr averaged data the segregated datasets were not large enough for the calibration analysis
237 ($N < 50$ for $PM_{2.5} > 100 \mu g m^{-3}$) so hourly averaged data were used. An alternative calibration was
238 developed using the hourly averaged PDM co-location data ($PM_{2.5,corr} = 111 + 0.596 * PM_{2.5, Clarity} -$
239 $0.861 * T - 0.801 * RH$, $RMSE = 27.8 \mu g m^{-3}$, $NRMSE = 0.0732 \mu g m^{-3}$). The piecewise calibration
240 model showed improved performance for $PM_{2.5} < 100 \mu g m^{-3}$ ($RMSE = 16.5 \mu g m^{-3}$, $NRMSE =$

241 **Table 3.** Calibration results for RBU and PDM co-located Clarity Monitor/WBPCB pairs on a 24
 242 hr average basis. RMSE: root mean squared error. RF: random forest regression. MLR: Multiple
 243 linear regression. PM_{2.5} is in units of $\mu\text{g m}^{-3}$, temperature is in degrees Celsius and relative
 244 humidity is in percent.

<i>Location</i>	<i>Uncorrected Clarity-WBPCB</i>	<i>RF</i>	<i>MLR</i>
RBU	RMSE: 27.1 $\mu\text{g m}^{-3}$ NRMSE: 0.070 R ² = 0.870	RMSE: 13.3 $\mu\text{g m}^{-3}$ NRMSE: 0.035 R ² = 0.962 <i>Feature importance</i> PM _{2.5} : 0.989 T: 0.00447 RH: 0.00642	RMSE: 15.3 $\mu\text{g m}^{-3}$ NRMSE: 0.040 R ² = 0.950 <i>Calibration model</i> PM _{2.5, corr} = 54.1+0.838*PM _{2.5, Clarity} +0.182*T-0.491*RH
PDM	RMSE: 32.6 $\mu\text{g m}^{-3}$ NRMSE: 0.086 R ² = 0.876	RMSE: 15.2 $\mu\text{g m}^{-3}$ NRMSE: 0.040 R ² = 0.936 <i>Feature importance</i> PM _{2.5} : 0.987 T: 0.00599 RH: 0.00676	RMSE: 10.2 $\mu\text{g m}^{-3}$ NRMSE: 0.027 R ² = 0.971 <i>Calibration model</i> PM _{2.5, corr} = 0.928+0.770*PM _{2.5, Clarity} +2.19*T-0.710*RH

245

246 0.165) but performance was worse for PM_{2.5}>100 $\mu\text{g m}^{-3}$ (RMSE = 44.5 $\mu\text{g m}^{-3}$, NRMSE = 0.091),
 247 and both models underperformed compared to the MLR model developed with the full 24-hr
 248 averaged PDM dataset (Table 3). Therefore, we opted not to use piecewise calibration.

249 In order to test the robustness of applying the calibrations developed at a single Clarity/RGM
 250 co-location site to another distant site (11.3 km apart) in the network, the following cross-
 251 calibration test was performed using the calibrations developed using the 24-hr averaged co-
 252 location data: the MLR calibration developed for the RBU site (Table 3) was applied to the PDM
 253 dataset, and the output was compared to the PDM WBPCB reference data. Likewise, the MLR
 254 calibration developed for PDM was applied to RBU and compared to the RBU WBPCB reference
 255 data. When the PDM MLR calibration was applied to the RBU dataset, agreement for the corrected
 256 data with the RBU WBPCB reference data improved (RMSE = 20.1 $\mu\text{g m}^{-3}$) compared to the raw
 257 Clarity data (RMSE = 27.1 $\mu\text{g m}^{-3}$), but not as much as when the locally developed calibration was
 258 applied (RMSE = 15.3 $\mu\text{g m}^{-3}$). Similar results were observed when the RBU MLR model was

259 applied to the PDM dataset: RMSE was equal to $24.2 \mu\text{g m}^{-3}$, improved compared to the raw Clarity
260 data (RMSE = $32.6 \mu\text{g m}^{-3}$), but not as much as when the locally developed MLR calibration was
261 applied (RMSE = $10.2 \mu\text{g m}^{-3}$). The cross-calibration corrected Clarity Monitor data for PDM and
262 RBU accurately diagnosed days as being in or out of attainment with the 24-hour mean Indian
263 NAAQS of $60 \mu\text{g m}^{-3}$, as compared to the WBPCB reference monitor data, 91% of the time. The
264 corrected data identified days with an India scale AQI of “poor” or worse ($\text{PM}_{2.5} > 90 \mu\text{g m}^{-3}$) in
265 agreement with the reference grade monitors 94% of the time.

266 Once the calibration method was established, the 24 hr average based MLR model derived from
267 the PDM dataset (Table 3) was applied to the entire sensor network to derive a corrected dataset.
268 Average corrected $\text{PM}_{2.5}$ values for the months of November 2018, January 2019, and April 2019,
269 as representative of the post-monsoon, winter, and spring/summer, are shown for each Clarity
270 Monitor in Table 4. Where data are not shown, no data are available for that month for that sensor.
271 Note that co-location data are not available for November 2018 and therefore the calibration was
272 not developed using data from that time period, however we expect the calibration model
273 performance for November to be similar to that for January since it is in the higher $\text{PM}_{2.5}$ loading
274 period. Averages for the 6 geographic zones and network-wide averages are also shown. Consistent
275 with regional trends for the Indo-Gangetic Plain (Guttikunda and Gurjar, 2012; Bhowmik, et al.
276 2021), pollution is highest in January, when citywide average $\text{PM}_{2.5}$ is $205 \pm 27 \mu\text{g m}^{-3}$, followed
277 by November, with an average value of $153 \pm 21 \mu\text{g m}^{-3}$. These values exceeded the NAAQS and
278 fell in the “Very Poor” category of the Indian AQI. $\text{PM}_{2.5}$ levels are significantly lower in April,
279 with an average of $47 \pm 8 \mu\text{g m}^{-3}$. $\text{PM}_{2.5}$ levels were highest at Howrah Bus Depot and lowest at
280 Camac Street (U.S. Consulate area). Among the zones, Howrah had the highest average $\text{PM}_{2.5}$
281 levels, although data were somewhat limited for that zone. There were only 3 sensors in the Howrah
282 zone. Ghosuri had limited data due to loss of the sensor after November 2018, and PDM was not

283 **Table 4.** Monthly average corrected Clarity PM_{2.5} data ($\mu\text{g m}^{-3}$) and standard deviation for
 284 November 2018, January 2019, and April 2019, months representing the post-monsoon, winter,
 285 and summer seasons in Kolkata. Data shown for each site, geographic zonal averages, and citywide
 286 average.

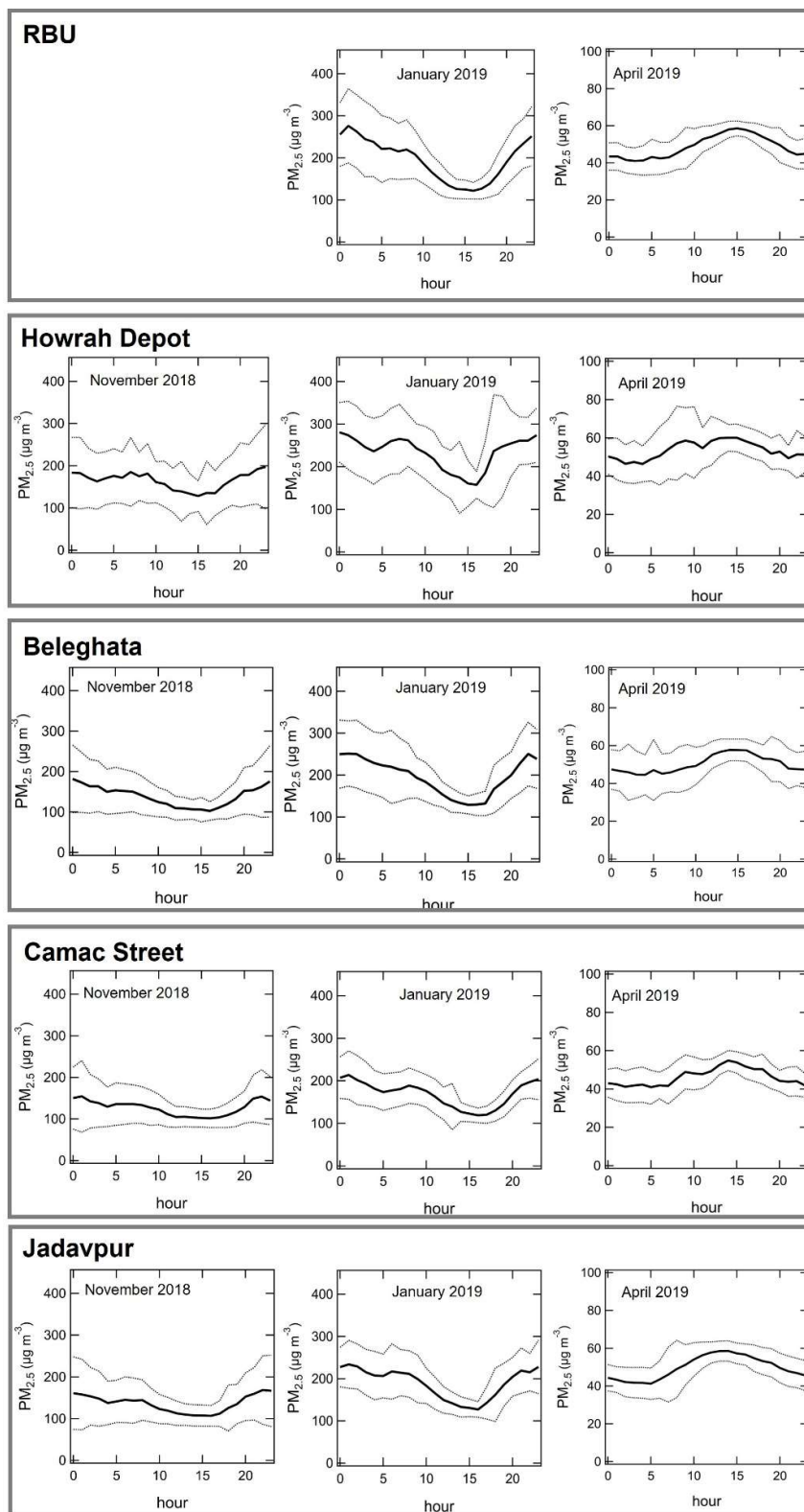
Code	Area	Nov 2018	Jan 2019	April 2019
Victoria Memorial	Central		189	41
Esplanade	Central	196	203	32
Marble Palace	Central	140	196	46
Camac Street	Central	130	166	41
Park Street Crossing	Central	142	192	42
Wellington	Central	150	216	51
Belegkata	East	149	201	52
SDF Building	East	126	162	33
Sealdah Sales Tax	East	176	257	58
Padmapukur (PDM)	Howrah		247	48
Howrah Bus Depot	Howrah	193	261	57
Ghusuri	Howrah	126		
Rabindra Bharati University (RBU)	North		204	48
Belgharia Police Station	North	162	203	57
Shyambazar	North	159	216	57
Baranagar Police Station	North	159		
Elgin & Lansdowne	South	141	188	48
Gariahat	South	141	183	45
Jadavpur (8B bus stand)	South	147	198	52
Rashbehari Crossing	South	162	225	
Millenium Park	West	153	207	48
<i>Howrah zone</i>		160	254	52
<i>North zone</i>		146	184	47
<i>West zone</i>		141	188	48
<i>East zone</i>		126	204	43
<i>South zone</i>		173	221	45
<i>Central zone</i>		146	196	46
AVERAGE		153 ± 21	205 ± 27	47±8

287

288 installed until WBPCB approval for the co-location, which was obtained in January 2019.

289 In order to investigate diurnal patterns in $PM_{2.5}$ across the network, the calibration developed
290 using the hourly averaged PDM co-location data ($PM_{2.5,corr} = 111 + 0.596*PM_{2.5,Clarity} - 0.861*T -$
291 $0.801*RH$, $RMSE = 27.8 \mu g m^{-3}$, $NRMSE = 0.0732 \mu g m^{-3}$) was applied to hourly average data for
292 the network, as shown in Figure 3. The diurnal trend varied seasonally. Generally, in November
293 and January, maximum $PM_{2.5}$ was observed in the late night hours (midnight-1 AM), with an
294 additional minor peak in the morning (7-10 AM), while in April, $PM_{2.5}$ varied more smoothly
295 throughout the day, with a maximum in the afternoon (1-4 PM). This post-monsoon/wintertime
296 diurnal pattern was consistent with what had been observed earlier for other large cities in the Indo-
297 Gangetic plain (Guttikunda and Gurjar, 2012; Gani et al. 2020). The nocturnal maximum in $PM_{2.5}$
298 could be attributed to low boundary layer height at night during post-monsoon and winter seasons.
299 Nighttime emissions such as residential burning for heating or cooking may also contribute. The
300 April pattern of an afternoon maximum with relatively little influence from morning and evening
301 traffic suggests regional non-traffic sources and/or secondary aerosol formation. We note this trend
302 observed in the corrected Clarity data, while unusual for cities in the IGP, is corroborated by the
303 WBPCB RGM data. Gani et al. (2020) reported that secondary components of PM_1 , consisting of
304 oxygenated organic aerosol, ammonium, nitrate, and sulfate, show a similar diurnal profile, with a
305 single peak in the afternoon, in Delhi during all seasons.

306 We further investigated the spatial variability in $PM_{2.5}$ by calculating the Pearson correlation
307 coefficient (r) between the datasets shown in Figure 3 (RBU, Howrah Depot, Belegkata, Camac
308 Street, and Jadavpur) for November, January, and April. The results are shown in Figure 4. $PM_{2.5}$
309 is highly linearly correlated among these sites for all seasons. This high level of correlation among
310 these sites with differing local sources underscores the importance of regional and secondary
311 sources of aerosol in Kolkata and Howrah. Although still highly correlated ($r \geq 0.79$) Howrah



312
 313 **Figure 3.** Hourly average corrected Clarity PM_{2.5} data for representative locations, for months
 314 representing the post-monsoon, winter, and summer seasons in Kolkata. Thin grey lines represent
 315 +/- one standard deviation.

NOVEMBER 2018					
	Howrah	Camac St.	Beleghata	RBU	PDM
Jadavpur	0.92	0.96	0.96		
PDM					
RBU					
Beleghata	0.89	0.96			
Camac St.	0.90				

JANUARY 2019					
	Howrah	Camac St.	Beleghata	RBU	PDM
Jadavpur	0.96	0.97	0.98	0.96	0.92
PDM	0.83	0.96	0.95	0.98	
RBU	0.87	0.97	0.98		
Beleghata	0.92	0.95			
Camac St.	0.88				

APRIL 2019					
	Howrah	Camac St.	Beleghata	RBU	PDM
Jadavpur	0.90	0.94	0.92	0.96	0.95
PDM	0.81	0.95	0.98	0.99	
RBU	0.83	0.95	0.98		
Beleghata	0.79	0.92			
Camac St.	0.88				

316
 317 **Figure 4.** Correlation between hourly average corrected PM_{2.5} measurements at different
 318 representative locations in the Clarity network, for months representing the post=monsoon, winter,
 319 and summer seasons in Kolkata.
 320

321 Depot showed lower correlation with the other sites, consistent with strong local sources.
 322 Correlation was slightly weaker in April as compared to November and January. The high degree
 323 of correlation of PDM with the other sites lend additional confidence in the choice to calibrate the
 324 network using the calibration developed based on the PDM co-location data.

325
 326 **4. DISCUSSION AND IMPLICATIONS**
 327

328 Air quality is a major public health issue in Kolkata. Previously published studies have shown
329 that chronic exposure to ambient air pollution in Kolkata adversely affects pulmonary and
330 cardiovascular health of its residents (Lahiri et al., 2000; Roy et al., 2001; Dutta et al., 2013). It is
331 important to be empowered with low cost tools and knowledge to assess local air pollution and the
332 associated health risks to advocate relevant policy measures in addressing environmental pollution
333 issues affecting local communities. Hence, we undertook this study to understand and validate the
334 performance of LCS in Kolkata, which could then be used to supplement existing RGM networks
335 for better air quality management.

336 During the study period, which covered the post-monsoon, winter, and spring/summer seasons
337 of 2018-2019, PM_{2.5} levels exceeded the NAAQS 45% of the time (and nearly 100% of the time
338 during the post-monsoon and winter months). This observation is consistent with other analyses of
339 PM_{2.5} in the IGP region (see, e.g., Zheng et al. 2018, Gani et al. 2020, and Gupta et al. 2022). The
340 highest average PM_{2.5} values in the network were observed at Howrah Bus Depot, suggesting that
341 idling buses may be a significant local source of PM_{2.5} that could be reduced with the introduction
342 of electric buses. The diurnal trends and high correlation among sites in different zones suggest
343 that regional and secondary sources are also very important. Winds are mostly north-westerly
344 during post-monsoon and winter seasons (October-February), bringing airmasses from the Indo-
345 Gangetic Plain, transporting regional haze as well as pollution from regional thermal power plants,
346 mining and steel industries. Based on Hybrid Single-Particle Lagrangian Integrated Trajectory
347 model (HYSPLIT) analysis, Mallik et al. (2014) showed that, during April, prevailing winds in
348 Kolkata generally come from the south (Bay of Bengal and coastal India) and transport occurs near
349 surface level. A future multi-season investigation involving aerosol composition and gas
350 measurements would provide necessary insight into the sources of PM_{2.5} in Kolkata.

351 Many of the Clarity Monitor sites in the network were near or on roadways or bus stands,
352 whereas the co-location sites, particularly RBU, were selected by WBPCB to be farther from roads
353 for security reasons and to characterize the urban background pollution. With the exception of
354 Howrah Depot, the difference in average $PM_{2.5}$ levels for the roadside vs. urban background sites
355 in each geographic zone is not consistently distinguishable within the error, even when filtering for
356 expected high traffic times (i.e., weekdays, 9-11 AM). However, some differences can be discerned
357 in the diurnal variation, e.g. the afternoon peak time during summer (Fig. 3). Sites located closer
358 to pollution sources, such as Howrah Depot, also showed greater day to day variability in measured
359 $PM_{2.5}$.

360 We have demonstrated the potential utility for a field-calibrated LCS network with
361 neighborhood-level spatial resolution to support air quality management efforts in Kolkata. This
362 study contributes to the growing body of work showing the promise of LCS in the South Asian
363 context (Zheng et al., 2018; Hagan et al., 2019; Crilley et al., 2020; Gupta et al., 2022; Kushawaha
364 et al., 2022). This study was the first deployment of Clarity devices in the Indian subcontinent.
365 Some practical limitations of application of the Clarity devices in Kolkata included issues with
366 charging and network connectivity, which resulted in data loss, the cost per unit, and the data
367 subscription charge. Supplementing the existing reference grade monitoring network with these
368 devices revealed spatiotemporal trends and insight into sources, which were not available with the
369 RGM network alone. Reasonable agreement between Clarity Monitors and WBPCB reference
370 grade monitors was obtained with in-field calibration, as tested by cross-calibration with two co-
371 located sensor/RGM pairs: the calibrated network accurately diagnosed days as being in or out of
372 attainment with the 24-hour mean Indian NAAQS of $60 \mu\text{g m}^{-3}$ with 91% accuracy, and correctly
373 assigned days to a category of the India scale Air Quality Index of “poor” or worse ($PM_{2.5} > 90 \mu\text{g}$
374 m^{-3}) with 94% accuracy.

375 **ACKNOWLEDGEMENTS**

376

377 Envirome Research acknowledges the World Bank for funding the deployment of the Clarity

378 Monitor network. AD, DMW, and VFM acknowledge the Columbia University Earth Institute for

379 support of this work under the Clean Air Toolbox for Cities initiative. DMW acknowledges NSF

380 OISE grant 2020677. We are grateful to the West Bengal Pollution Control Board for sharing data,

381 permitting sensor co-locations at monitoring sites, and helpful discussions. The authors are also

382 grateful to Sarbani Palit, Celeste McFarlane, Shahzad Gani, and Sean Wihera for helpful

383 discussions. Corrected Clarity monitor data will be made publicly available on PANGAEA

384 (www.pangaea.de) after acceptance. Regulatory instrument data from the West Bengal Pollution

385 Control Board are available through the CPCB Central Control Room for Air Quality Management

386 data dashboard (<https://app.cpcbcr.com>).

387

388 **REFERENCES**

389

390 Amegah, A.K. (2018). Proliferation of low-cost sensors. What prospects for air pollution

391 epidemiologic research in Sub-Saharan Africa? *Environ. Pollut.* 241 1132-1137.

392 <https://doi.org/10.1016/j.envpol.2018.06.044>

393 Apte. J.S., Brauer, M., Cohen, A.J., Ezzati, M., Pope III, C.A. (2018). Ambient PM_{2.5} Reduces

394 Global and Regional Life Expectancy. *Environ. Sci. Technol. Lett.* 5, 546-551.

395 <https://doi.org/10.1021/acs.estlett.8b00360>

396 Bhowmik, H.S., Naresh, S., Bhattu, D., Rastogi, N., Prevot, A.S.H., Tripathi, S.N. (2021).

397 Temporal and spatial variability of carbonaceous species (EC; OC; WSOC and SOA) in

398 PM_{2.5} aerosol over five sites of Indo-Gangetic Plain. *Atmos. Pollut. Res.* 12(1) 375-390.

399 <https://doi.org/10.1016/j.apr.2020.09.019>

400 Cohen, A.J., Brauer, M., Burnett, R., Anderson, H.R., Frostad, J., Estep, K., Balakrishnan, K.,

401 Brunekreef, B., Dandona, L., Feigin, V., Freedman, G., Hubbell, B., Jobling, A., Kan, H.,

402 Knibbs, L., Liu, Y., Martin, R., Morawska, L., Pope, C.A., Shin, H., Straif, K., Shaddick,

403 G., Thomas, M., van Dingenen, R., van Donkelaar, A., Vos, T., Murray, C.J.L.,

404 Forouzanfar, M.H. T. (2017) Estimates and 25-year trends of the global burden of disease

405 attributable to ambient air pollution: An analysis of data from the Global Burden of

406 Diseases Study 2015. *Lancet* 389, 10082, 1907-1918. <https://doi.org/10.1016/S0140->

407 [6736\(17\)30505-6](https://doi.org/10.1016/S0140-6736(17)30505-6)

408 CPCB Central Control Room for Air Quality Management - All India <https://app.cpcbcr.com>

409 (Accessed February 2022).

410 Crilley, L.R., Singh, A., Kramer, L.J., Shaw, M.D., Alam, M.S., Apte, J.S., Bloss, W.J., Ruiz,

411 L.H., Fu, P., Fu, W., Gani, S., Gatari, M., Ilyinskaya, E., Lewis, A.C., Ng'ang'a, D., Sun,

412 Y., Whitty, R.C.W., Yue, S., Young, S., Pope, F.D. (2020) Effect of aerosol composition

413 on the performance of low-cost optical particle counter correction factors. *Atmos. Meas.*
414 *Tech.*, 13, 1181–1193. <https://doi.org/10.5194/amt-13-1181-2020>

415 Di Antonio, A., Popoola, O.A.M., Ouyang, B., Saffell, J., Jones, R.L. (2018) Developing a
416 Relative Humidity Correction for Low-Cost Sensors Measuring Ambient Particulate
417 Matter. *Sensors* 18(9), 2790 <https://doi.org/10.3390/s18092790>

418 Dutta, A. and Ray, M.R. (2013) Increased cardiovascular risk due to systemic inflammatory
419 changes and enhanced oxidative stress in urban Indian women. *Air Qual. Atmos. Health*
420 6(2), 501- 508. <https://doi.org/10.1007/s11869-012-0189-0>

421 Gani, S., Bhandari, S., Patel, K., Seraj, S., Soni, P., Arub, Z., Habib, G., Ruiz, L.H., Apte, J.S.
422 (2020) Particle number concentrations and size distribution in a polluted megacity: the
423 Delhi Aerosol Supersite study. *Atmos. Chem. Phys.* 20, 8533-8549.
424 <https://doi.org/10.5194/acp-20-8533-2020>

425 Giordano, M.R., Malings, C., Pandis, S.N., Presto, A.A., McNeill, V.F., Westervelt, D.M.,
426 Beekmann, M., Subramanian, R. (2021) From Low-cost Sensors to High-Quality Data: A
427 Summary of Challenges and Best Practices for Effectively Calibrating Low-Cost
428 Particulate Matter Mass Sensors. *J. Aerosol Sci.* 158, 105833
429 <https://doi.org/10.1016/j.jaerosci.2021.105833>

430 Gupta, P., Doraiswamy, P., Reddy, J., Balyan, P., Dey, S., Chartier, R., Khan, A., Riter, K.,
431 Feenstra, B., Levy, R.C., Tran, N.N.M., Pikelnaya, O., Selvaraj, K., Ganguly, T.,
432 Ganesan, K. (2022) Low-Cost Air Quality Sensor Evaluation and Calibration in
433 Contrasting Aerosol Environments *Atmos. Meas. Tech. Discuss.* [preprint],
434 <https://doi.org/10.5194/amt-2022-140>

435 Guttikunda, S.K. and Gurjar, B.R. (2012) Role of meteorology in seasonality of air pollution in
436 megacity Delhi, India. *Environ. Monit. Assess.* 184, 3199-3211
437 <https://doi.org/10.1007/s10661-011-2182-8>

438 Hagan, D.H., Gani, S., Bhandari, S., Patel, K., Habib, G., Apte, J.S., Ruiz, L.H., Kroll, J.H. (2019)
439 Inferring Aerosol Sources from Low-Cost Air Quality Sensor Measurements: A Case Study
440 in Delhi, India. *Environ. Sci. Technol. Lett.* 6 (8) 467-472. 10.1021/acs.estlett.9b00393

441 Hagler, G.S.W., Williams, R., Papapostolou, V., Polidori, A. (2018) Air Quality Sensors and
442 Data Adjustment Algorithms: When Is It No Longer a Measurement? *Environ. Sci.*
443 *Technol.* 52, 10, 5530–5531. <https://doi.org/10.1021/acs.est.8b01826>

444 Jayaratne, R., Liu, X., Thai, P., Dunbabin, M., Morawska, L. (2018) The influence of humidity
445 on the performance of a low-cost air particle mass sensor and the effect of atmospheric
446 fog. *Atmos. Meas. Tech.*, 11, 4883–4890. <https://doi.org/10.5194/amt-11-4883-2018>

447 Kushawaha, M., Sreekanth, V., Upadhyaya, A.R., Agrawal, P., Apte, J.S., Marshall, J.D. (2022) Bias
448 in PM_{2.5} measurements using collocated reference-grade and optical instruments. *Environ.*
449 *Monit. Assess.* 194:610. <https://doi.org/10.1007/s10661-022-10293-4>

450 Lahiri, T.; Roy, S.; Ganguly, S.; Ray, M.R.; Lahiri, P. (2000) Air pollution in Calcutta elicits
451 adverse pulmonary reaction in children. *Ind. J. Med. Res.* 112, 21–26.

452 Malings, C.; Tanzer, R.; Hauryliuk, A.; Saha, P. K.; Robinson, A. L.; Presto, A. A.; Subramanian,
453 R. (2020) Fine particle mass monitoring with low-cost sensors: Corrections and long-term
454 performance evaluation. *Aerosol Sci. Technol.*, 54:2, 160-174,
455 <https://doi.org/10.1080/02786826.2019.1623863>

456 Mallik, C., Ghosh, D., Ghosh, D., Sarkar, U., Lal, S., Venkataramani, S. (2014) Variability of
457 SO₂, CO, and light hydrocarbons over a megacity in Eastern India: effects of emissions

458 and transport. *Environ. Sci. Pollut. Res.* 21, 8692–8706. <https://doi.org/10.1007/s11356->
459 014-2795-x

460 McFarlane, C., Isevlambire, P.K., Lumbuenamo ,R.S., Dhammapala, R., Jin, X., McNeill, V.F.,
461 Malings, C., Subramanian, R., Westervelt, D.M. (2021a) First ambient measurements of
462 PM_{2.5} in Kinshasa, Democratic Republic of Congo and Brazzaville, Republic of Congo
463 using field-calibrated low cost sensors, *Aerosol Air Qual. Res.* 21 (7) 200619.
464 <https://doi.org/10.4209/aaqr.200619>

465 McFarlane,C., Raheja, G., Malings C., Appoh, E.K.E., Hughes A.F., Westervelt, D.M. (2021b)
466 Application of Gaussian Mixture Regression for the Correction of Low Cost PM_{2.5}
467 Monitoring Data in Accra, Ghana *ACS Earth Space Chem.* 5 (9) 2268-2279.
468 <https://doi.org/10.1021/acsearthspacechem.1c00217>

469 McNeill, V.F. (2019) Addressing the Global Air Pollution Crisis: Chemistry’s Role. *Trends*
470 *Chem.* 1 (1), 5-8. <https://doi.org/10.1016/J.TRECHM.2019.01.005>

471 McNeill, V.F. and Nunes, J.F. (2017) “India’s Air Pollution Crisis: By the Numbers,” *Huffpost*
472 *India*, October 26, 2017 [https://www.huffpost.com/archive/in/entry/indias-air-pollution-](https://www.huffpost.com/archive/in/entry/indias-air-pollution-crisis-by-the-numbers_in_5c12c6c3e4b0d73db4b48126)
473 [crisis-by-the-numbers_in_5c12c6c3e4b0d73db4b48126](https://www.huffpost.com/archive/in/entry/indias-air-pollution-crisis-by-the-numbers_in_5c12c6c3e4b0d73db4b48126)

474 Müller, A. and Guido, S. (2017) *Introduction to Machine Learning with Python: A Guide for*
475 *Data Scientists*. O’Reilly.

476 Pinder. R.W., Klopp, J.M., Kleiman, G., Hagler, G.S.W., Awe, Y., Terry, S. (2019) Opportunities
477 and challenges for filling the air quality data gap in low- and middle-income countries.
478 *Atmos. Environ.* 215, 116794. <https://doi.org/10.1016/j.atmosenv.2019.06.032>

479 Raheja, G., Sabi, K., Sonla, H., Gbedjangni, E.K., McFarlane, C.M., Hodoli C.G., Westervelt,
480 D.M. (2022) A Network of Field-Calibrated Low-Cost Sensor Measurements of PM_{2.5} in

481 Lomé, Togo. *ACS Earth Space Chem.* 6(4) 1011-1021.
482 <https://doi.org/10.1021/acsearthspacechem.1c00391>

483 Roy S, Ray MR, Basu C, Lahiri P, Lahiri T. (2001) Abundance of siderophages in sputum:
484 indicator of an adverse lung reaction to air pollution. *Acta Cytol.* Nov-Dec; 45 (6), 958-
485 964. <https://doi.org/10.1159/000328371>

486 Sethuraman S., Das Y., McNeill, V.F. (2021) “INDIA’S AIR POLLUTION BY THE
487 NUMBERS: 2019–2020 ANALYSIS” *Medium*, October 8, 2021
488 [https://aqtoolbox.medium.com/indias-air-pollution-by-the-numbers-2019-2020-analysis-](https://aqtoolbox.medium.com/indias-air-pollution-by-the-numbers-2019-2020-analysis-7d1082316305)
489 [7d1082316305](https://aqtoolbox.medium.com/indias-air-pollution-by-the-numbers-2019-2020-analysis-7d1082316305)

490 WBPCB (2018) CAAQM Technical Specifications
491 https://www.wbpcb.gov.in/writereaddata/files/Bid_CAAQMTechnicalBid2018_5.pdf

492 World Bank (2021) ESMAP IMPACT report “INDIA: TRANSITION TO ELECTRIC
493 VEHICLES PUTS KOLKATA ON THE ROAD TO CLEAN TRANSPORT”
494 [https://documents1.worldbank.org/curated/en/479341609914443074/pdf/India-Transition-](https://documents1.worldbank.org/curated/en/479341609914443074/pdf/India-Transition-to-Electric-Vehicles-Puts-Kolkata-on-the-Road-to-Clean-Transport.pdf)
495 [to-Electric-Vehicles-Puts-Kolkata-on-the-Road-to-Clean-Transport.pdf](https://documents1.worldbank.org/curated/en/479341609914443074/pdf/India-Transition-to-Electric-Vehicles-Puts-Kolkata-on-the-Road-to-Clean-Transport.pdf)

496 WHO, 2021. Ambient (outdoor) air pollution. [https://www.who.int/news-room/fact-](https://www.who.int/news-room/fact-sheets/detail/ambient-(outdoor)-air-quality-and-health)
497 [sheets/detail/ambient-\(outdoor\)-air-quality-and-health](https://www.who.int/news-room/fact-sheets/detail/ambient-(outdoor)-air-quality-and-health) (Accessed on December 19, 2022)

498 Zheng, T., Bergin, M.H., Johnson, K.K., Tripathi, S.N., Shirodkar, S., Landis, M.S., Sutaria, R.
499 Carlson, D.E. (2018) Field evaluation of low-cost particulate matter sensors in high- and
500 low-concentration environments *Atmos. Meas. Tech.*, 11, 4823–4846.
501 <https://doi.org/10.5194/amt-11-4823-2018>

502 Zimmerman, N., Presto, A.A., Kumar, S.P.N., Gu, J. Hauryliuk, A., Robinson, E.S., Robinson,
503 A.S., Subramanian, R. (2018) A Machine Learning Calibration Model Using Random

504 Forests to Improve Sensor Performance for Lower-Cost Air Quality Monitoring. *Atmos.*
505 *Meas. Tech.* 11, 291-313. <https://doi.org/10.5194/amt-11-291-2018>